Journal of Controlled Release 215 (2015) 1–11

Contents lists available at ScienceDirect

Journal of Controlled Release

journal homepage: www.elsevier.com/locate/jconrel

Circumventing the blood–brain barrier: Local delivery of cyclosporin A stimulates stem cells in stroke-injured rat brain

Anup Tuladhar [a,e], Cindi M. Morshead [a,b,e], Molly S. Shoichet [a,c,d,e,*]

[a] Institute of Biomaterials and Biomedical Engineering, University of Toronto, 164 College Street, Toronto, ON M5S 3G9, Canada
[b] Department of Surgery, University of Toronto, 149 College Street, Toronto, ON M5S 3E1, Canada
[c] Department of Chemical Engineering and Applied Chemistry, University of Toronto, 200 College Street, Toronto, ON M5S 3E5, Canada
[d] Department of Chemistry, University of Toronto, 80 St. George Street, Toronto, ON M5S 3H6, Canada
[e] Donnelly Centre for Cellular and Biomolecular Research, University of Toronto, 160 College Street, Toronto, ON M5S 3E1, Canada

ARTICLE INFO

Article history:
Received 27 April 2015
Received in revised form 19 June 2015
Accepted 21 July 2015
Available online 27 July 2015

Keywords:
Hydrogel
Stroke
Drug delivery
Cyclosporin A
Neural stem progenitor cell
Blood brain barrier

ABSTRACT

Drug delivery to the central nervous system is limited by the blood–brain barrier, which can be circumvented by local delivery. In applications of stroke therapy, for example, stimulation of endogenous neural stem/progenitor cells (NSPCs) by cyclosporin A (CsA) is promising. However, current strategies rely on high systemic drug doses to achieve small amounts of CsA in the brain tissue, resulting in systemic toxicity and undesirable global immunosuppression. Herein we describe the efficacy of local CsA delivery to the stroke-injured rat brain using an epicortically injected hydrogel composed of hyaluronan and methylcellulose (HAMC). CsA was encapsulated in poly(lactic-co-glycolic acid) microparticles dispersed in HAMC, allowing for its sustained release over 14 days in vivo. Tissue penetration was sufficient to provide sustained CsA delivery to the sub-cortical NSPC niche. In comparison to systemic delivery using an osmotic minipump, HAMC achieved higher CsA concentrations in the brain while significantly reducing drug exposure in other organs. HAMC alone was beneficial in the stroke-injured rat brain, significantly reducing the stroke infarct volume relative to untreated stroke-injured controls. The combination of HAMC and local CsA release increased the number of proliferating cells in the lateral ventricles — the NSPC niche in the adult brain. Thus, we demonstrate a superior method of drug delivery to the rat brain that provides dual benefits of tissue protection and endogenous NSPC stimulation after stroke.

1. Introduction

The development of treatments for central nervous system (CNS) disorders is severely hindered by the lack of effective therapeutic delivery systems. Drug delivery to the brain is impeded by the blood brain barrier (BBB) lining the cerebrovasculature that prevents transport of many systemically administered molecules [1]. To achieve therapeutic levels and efficacy, many pre-clinical drug studies require undesirable BBB disruption [2–4] or high dosages [4–6] that produce systemic side effects and toxicity. Circumventing the BBB using local delivery can overcome these challenges. However, current local delivery methods are limited to highly invasive intracranial or intracerebroventricular (ICV) drug infusion with a catheter, causing further tissue damage to the stroke-injured brain [7]. Additionally, clinical use of this strategy with the Ommaya reservoir is associated with a high risk of cerebral infections [8]. A minimally invasive method for local drug delivery to the brain is necessary.

A physically crosslinked hydrogel comprised of hyaluronan (HA) and methylcellulose (MC), HAMC, provides minimally-invasive local drug delivery. It is injectable, gels rapidly at physiological temperatures, and is bioresorbable [9]. HAMC can be used alone [10–13] or in combination with drug-loaded polymeric particles [7,14,15] to deliver therapeutics to the CNS. In the mouse brain, an epi-cortical delivery strategy was used to inject HAMC for local drug release of bioactive drug without damage to brain tissue [7,12,13,15] (Fig. 1). One key question is whether this strategy will be useful in larger brains. In a first step to answering this question we investigated local drug delivery with HAMC in the stroke-injured rat brain, which is four times the volume of the mouse brain.

Stroke affects 15 million people worldwide annually, leaving one third with brain damage and permanent disabilities [16]. Currently, there is no treatment that repairs the damaged brain tissue. Resident neural stem cells and progenitor cells (NSPCs) in the adult brain hold promise for endogenous tissue repair after stroke [17,18]. NSPCs are constitutively active and form new neurons capable of integrating into existing tissue [19]. Although NSPCs respond to stroke, transiently increasing proliferative activity and migrating toward the lesion [20,21], the majority undergo cell death [22,23] and have limited neurogenesis [24]. Stimulating endogenous adult forebrain NSPCs, which are located

* Corresponding author at: Department of Chemical Engineering and Applied Chemistry, University of Toronto, 200 College Street, Toronto, ON M5S 3E5, Canada.
E-mail address: molly.shoichet@utoronto.ca (M.S. Shoichet).

http://dx.doi.org/10.1016/j.jconrel.2015.07.023
0168-3659/

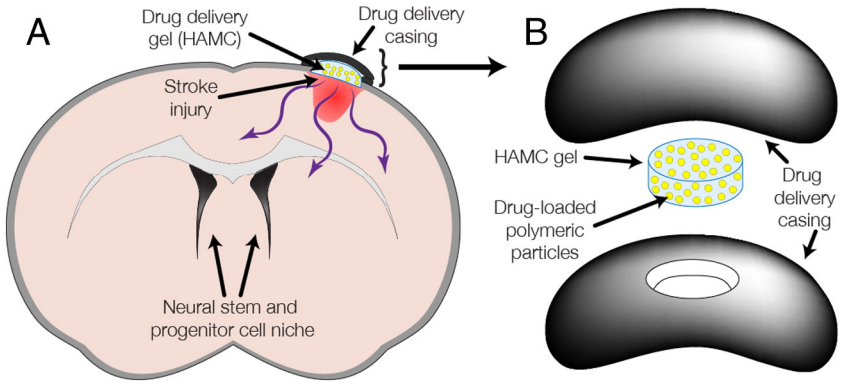

Fig. 1. Sustained local delivery to the brain can be achieved using drug-loaded polymeric particles suspended in hyaluronan/methylcellulose (HAMC) hydrogel. (A) Coronal view of stroke-injured brain with drug delivery system shows that HAMC is injected directly onto the cortex. (B) Drug delivery system in expanded view shows that HAMC is held in place by both gelation and a casing comprised of polycarbonate discs.
Figure adapted with permission from [12]; copyright 2011 Elsevier.

in the subependyma lining the lateral ventricles, is possible with a number of therapeutics [25], including: epidermal growth factor [26,27], human chorionic gonadotropin [28], erythropoietin [27,28], glial cell-derived neurotrophic factor [29], vascular endothelial growth factor [30] and cyclosporin A (CsA) [31,32].

CsA, a 1.2 kDa hydrophobic polypeptide, directly acts on NSPCs by promoting their survival and increasing the size of the NSPC pool in vitro and in vivo [32,33]. Indeed, systemic CsA administration for 7 to 14 days significantly increases the pool of NSPCs in both the brain and spinal cord [32,34]. After stroke, adult mice treated with CsA show tissue regeneration and sensorimotor functional recovery [31,32]. Moreover, CsA has neuroprotective effects in the brain [2,35,36], with phase II clinical trials completed for stroke (NCT01527240) and traumatic brain injury (TBI) (NCT01825044). The combination of regenerative and protective mechanisms makes CsA a promising molecule for stroke treatment. Although CsA crosses the BBB to a limited degree [37,38], its diffusion is severely restricted by efflux transporters, along the luminal wall of the BBB [39,40]. Additionally, systemic toxicity and global immunosuppression associated with high CsA doses warrant the use of local delivery [41]. Herein we report the first demonstration of epi-cortical local drug delivery to the stroke-injured rat brain. Using CsA-loaded poly(lactic-co-glycolic acid) (PLGA) microparticles dispersed in HAMC, we measured CsA diffusion and tissue penetration in the stroke-injured rat brain for 14 days. In this comprehensive study, local drug delivery with HAMC was compared to conventional systemic delivery with a subcutaneous osmotic minipump, assessing CsA concentration in the brain, delivery efficiency and organ exposure. Moreover, we evaluated the efficacy of local CsA release from HAMC in the stroke-injured rat brain in terms of its effect on stroke infarct volume and endogenous NSPC stimulation.

2. Materials and methods

All reagents were purchased from Sigma-Aldrich (Oakville, ON, Canada), unless specified otherwise.

2.1. CsA encapsulation in PLGA microparticles

CsA (Cat.# C-6000, LC Laboratories, Woburn, MA, USA) was encapsulated in PLGA (acid-terminated 50:50, MW 7000–17,000, Cat.# 71989) microparticles using a single-phase oil/water emulsion solvent evaporation technique, as described previously [15]. Blank PLGA particles were similarly prepared without the addition of CsA in the organic phase. Both particles were sterilized with 2.5 MRad of gamma radiation. The mean particle size was 14.7 μm, as measured by laser diffraction (Malvern Mastersizer 2000, Malvern, Worcestershire, UK). An average drug loading of 73 μg CsA/mg particle and encapsulation efficiency of 80.3% was achieved post-sterilization.

2.2. Preparation of sterile HA and MC

Sterile HA (1.4–1.8 × 10^6 g/mol, Pharmagrade 150 sodium hyaluronate, NovaMatrix, Sandvika, Norway), and MC (3.4 × 10^5 g/mol, Cat.# SM-4000-C, Shin Etsu, Chiyoda-ku, Tokyo, Japan) were independently prepared by dissolution in ddH_2O (Millipore Milli-RO 10 Plus and Milli-Q UF Plus at 18 MΩ resistivity, Millipore, Bedford, MA, USA), filtration through 0.2 μm filters and lyophilization (Labconco, Kansas City, MO, USA), all under sterile conditions. The sterile polymers were stored at −20 °C until use.

2.3. Preparation of drug delivery gel

The drug delivery gel was prepared under sterile conditions in a biosafety level 2 laminar flow hood or sealed from the external environment when necessary. The final composite contained 1.4 wt.% HA, 3 wt.% MC and 10 wt.% CsA or blank PLGA particles. First, a 2× concentrated mixture of HAMC (2.8 wt.% HA, 6 wt.% MC) was prepared by sequential dispersion in sterile artificial cerebrospinal fluid (aCSF: 148 mM NaCl, 3 mM KCl, 0.8 mM $MgCl_2$, 1.4 mM $CaCl_2$, 1.5 mM Na_2HPO_4, 0.2 mM NaH_2PO_4 in ddH_2O, pH adjusted to 7.4, filter sterilized at 0.2 μm) using a dual asymmetric centrifugal mixer (Flacktek Inc., Landrum, SC, USA). The gel was kept at 4 °C for 6–8 h to allow dissolution and centrifuged at 16,000 *g* for 10 min to remove any air bubbles. Sterile CsA particles were re-suspended at 20 wt.% in sterile aCSF, using a bath sonicator for 5 min to break up any aggregates. Equal volumes of 20 wt.% particles in aCSF and 2× HAMC were combined, dispersed using the dual asymmetric centrifugal mixer and kept at 4 °C overnight. The HAMC composite was loaded into autoclaved 100 μL Hamilton needles with an 18G tip (Model 1701 RN, Hamilton, Reno, NV, USA).

2.4. Animal approval

All animal work was carried out in accordance with the Guide to the Care and Use of Experimental Animals (Canadian Council on Animal Care) and approved by the Animal Care Committee at the University of Toronto. 10–14 week-old male Long–Evans rats were used (Charles River, QC, Canada). A total of 58 animals were used in these studies.

2.5. Endothelin-1 stroke

Stroke surgeries were carried out as described previously [42]. Anteroposterior (AP) and mediolateral (ML) coordinates are measured

relative to bregma; dorsoventral (DV) coordinates are relative to the skull surface. Rats were anesthetized with isoflurane, shaved and placed into a Kopf stereotaxic instrument. An off-midline incision was made in the scalp and a 2.7 mm burr hole centered around AP + 1.15 mm and ML + 2.5 mm was made using a trephine drill bit (Cat.# 18004-27, Fine Science Tools Inc., Vancouver, BC, Canada). Endothelin-1 (Et-1) (400 pmol/μL in ddH_2O, Cat.# 05-23-3800, Calbiochem, Gibbstown, NJ, USA) was injected using a 10 μL Hamilton syringe with a 26G, 45° bevel needle (Model 1701 RN, Hamilton) controlled with an automated injector (Pump 11 Elite Nanomite, Harvard Apparatus, Saint-Laurent, QC, Canada). Injections were made into the following coordinates in the motor cortex:

1) AP + 2.3, ML + 2.5 mm, DV −2.3 mm
2) AP 0 mm, ML + 2.5 mm, DV −2.3 mm

For each injection, the needle was lowered to −2.4 mm DV and then raised DV +0.1 mm, for a final coordinate of DV −2.3 mm. The needle was left to equilibrate for 1 min, after which 2 μL Et-1 was injected at 0.5 μL/min, with a 1 min pause after the first 1 μL. After completion of injections the needle was left to equilibrate for 3 min and then slowly withdrawn.

2.6. Drug delivery gel implantation

Animals receiving the HAMC hydrogel had a durectomy directly prior to Et-1 injections. A surgical microscope was used to aid the micro-dissection, taking care not to remove the pial vessel layer. After Et-1 injections, a curved 5.9 mm polycarbonate disk (Fig. 1B, bottom) [12] with a 2.7 mm opening was fixed over the burr hole with bone glue (Loctite 454, Henkel Corporation, Rocky Hill, CT, USA). 6 μL of HAMC gel with PLGA microparticles were directly injected onto the brain's cortical surface, filling the space formed by the skull and disk (Fig. 1A). A second 5.9 mm polycarbonate disk with no opening (Fig. 1B, top) was placed over top of the first disk and the skin was sutured closed. The gel used for CsA + HAMC treated animals contained CsA-loaded PLGA microparticles with 43.55 μg CsA per animal. The gel used for HAMC treated animals contained blank PLGA microparticles.

Untreated control animals received identical procedures (stroke, durectomy and drug delivery casing installation) but had no gel injected onto the brain (Fig. 1B).

2.7. Minipump implantation

For animals receiving a subcutaneous minipump, stroke surgeries were carried out as above. After the last Et-1 injection, a 5.9 mm polycarbonate disk with no opening (Fig. 1B, bottom) was fixed over the burr hole to close off the opening. A small incision was made over the right shoulder and a 14-day, 0.425 μL/h minipump (Alzet Model 2002, Durect Corporation, Cupertino, CA, USA) loaded with 425 mg/mL CsA in conventional 65% ethanol, 35% Cremophor EL was inserted into the subcutaneous space and the incision sutured closed.

2.8. Analysis of CsA concentration in the brain

Animals were sacrificed 1, 4, 7 and 14 days after gel or minipump implantation and the brains were snap frozen in $CO_{2(s)}$ cooled isopentane and stored at −80 °C. Six 1-mm coronal sections surrounding the stroke lesion were prepared from frozen brains using a McIlwain tissue chopper (Mickle Laboratory Engineering Company, Surrey, UK). Dorsoventral sections 0.5 mm thick were collected from each coronal slice using a Leica CM3050S cryostat system operating at −25 °C. Sections at the same depth from the cortical surface were combined in 2 mL polystyrene microtubes. Tubes were weighed before and after sample collection to determine the mass of brain tissue contained therein. Before tissue homogenization, 5 × 1.0-mm diameter zirconia beads (Cat.# 11079110zx, Biospec Products, Bartlesville, OK, USA), 50 μL of 325 mM $ZnSO_4$ and 50 μL of methanol (MeOH, HPLC grade, Caledon Labs, Georgetown, CA, USA) containing 25 ng/mL FK-506 (F-4900, LC Laboratories) as an internal standard (IS) were added to the tubes. Tissue was homogenized for 1.5 min with a Mini-beadbeater 16 (Biospec Products), cooled on ice for 1.5 min, and homogenized again for 1.5 min. CsA was extracted by adding 150 μL acetonitrile (ACN, HPLC grade, Caledon Labs), homogenizing tissue for 1 min, centrifuging at 4 °C for 10 min at 16,000 *g* and removing the supernatant for analysis. CsA was detected by high pressure liquid chromatography tandem mass spectrometry (HPLC–MS/MS), as described previously [15]. CsA standards in MeOH with IS (final concentration: 0.25 to 100 ng/mL) were spiked in clean, uninjured brain tissue and exacted through the same extraction procedure. The amount of CsA at each depth was divided by the mass of brain tissue to determine the concentration.

2.9. Analysis of CsA concentration in organs

Sections of heart, lung, liver, kidney, and spleen were taken from animals treated with CsA from HAMC or systemic minipump for 7 days. Samples were collected in 2 mL polystyrene microtubes that were weighed before and after sample collection to determine sample mass. Before tissue homogenization, 20 × 1.0-mm diameter zirconia beads, 200 μL of 325 mM $ZnSO_4$ and 200 μL of MeOH containing 25 ng/mL IS were added to the tubes. Tissue was homogenized for 1.5 min, cooled on ice for 1.5 min, and homogenized again for 1.5 min. CsA was extracted by adding 600 μL ACN, homogenizing tissue for 1 min, centrifuging at 4 °C for 15 min at 16,000 *g* and the supernatant analyzed with HPLC–MS/MS. CsA standards in MeOH with IS (final concentration: 0.25 to 50 ng/mL) were exacted through the same extraction procedure. The amount of CsA detected was divided by the mass of organ sample collected to determine the concentration.

2.10. Analysis of CsA released from HAMC in vivo

HAMC gels recovered from animals at 1, 4, 7 and 14 days post-implantation were digested in 1 mL ACN with IS (250 ng/mL) overnight at 4 °C with agitation. Samples were then centrifuged at 4 °C for 10 min at 16,000 *g*, diluted 100× in ACN with IS (250 ng/mL) and mass of CsA remaining in the gel was detected with HPLC–MS/MS. Standards (50 to 1000 ng/mL) were prepared using CsA powder exacted through the same digestion procedure. The amount of CsA released was calculated as the difference between the amount initially delivered and the amount remaining in the gel.

2.11. Calculation of CsA delivery efficiency to the brain

CsA delivery efficiency was calculated as the total amount of drug found in the region of brain-tissue analyzed at each time point (6 × 1-mm coronal sections in ipsilateral hemisphere surrounding the stroke lesion) as a percentage of the total CsA administered to the animal. For HAMC, this was the total CsA found in the 6 μL of gel implanted (43.55 μg). For systemic delivery with minipumps, this was the total CsA administered over 14 days (60,690 μg). The relative increase in delivery efficiency with HAMC vs. systemic was calculated as the ratio of the delivery efficiency of the two systems at each time point, with the highest increase (876,000 times) at 1 day post-stroke and lowest increase (2600 times) at 14 days post-stroke.

2.12. Brain tissue preparation for histological analysis

At specific time points, animals were transcardially perfused with saline followed by 4% paraformaldehyde (PFA). Brains were extracted and fixed in 4% PFA at 4 °C overnight, followed by cryoprotection in 10 → 20 → 30% sucrose. Cryoprotected brains were snap frozen and coronal sections cryosectioned at 25 μm slice thickness.

2.13. Immunohistochemistry

Sections stained for Ki67 and doublecortin (DCX) were permeabilized for 30 min (1% Triton X-100 in PBS), blocked for 30 min (0.1% Triton X-100 and 5% BSA in PBS) and incubated with mouse anti-human Ki-67 (0.625 μg/mL, Cat.# 550609, BD Pharmingen, Mississauga, ON, Canada) and rabbit anti-mouse DCX (2.5 μg/mL, ab18723, Abcam, Cambridge, MA, USA) primary antibodies at 4 °C overnight. Sections were then washed 3 times, 5 min each time, in PBS and incubated in AlexaFluor 488 goat anti-rabbit (10 μg/mL, Cat.# A-11034, Invitrogen Inc., Burlington, ON, Canada) and AlexaFluor 568 goat anti-mouse (10 μg/mL, Cat.# A-11030, Invitrogen Inc.) for 1 h at 25 °C. Sections were washed 3 times in PBS, mounted with Vectashield containing DAPI (H-1200, Vector Laboratories, Burlington, ON, Canada) and sealed.

Sections stained for NeuN were permeabilized for 15 min (1% Triton X-100 in PBS), blocked for 15 min (0.1% Triton X-100 and 5% BSA in PBS) and incubated with mouse anti-NeuN (2.5 μg/mL, MAB377, Millipore Inc., Billerica, MA, USA) primary antibody at room temperature for 1 h. Sections were then washed 3 times, 5 min each time, in PBS and incubated in AlexaFluor 568 goat anti-mouse (10 μg/mL) for 1 h at 25 °C. Sections were washed 3 times in PBS, mounted with Vectashield containing DAPI and sealed.

2.14. Infarct volume measurement

Coronal $NeuN^+$ stained sections between AP +5 mm and AP −1.0 mm relative to bregma and spaced 250–500 μm apart were assessed for infarct size. Z-stack images (5 μm step size) were taken with a 20× objective on a confocal microscope with a motorized stage, transformed into maximum projection images and stitched together. A total of 13–15 sections were assessed per animal. Animals with an insufficient number of unfolded sections were removed from analysis a priori (final group sizes: n = 5 for untreated, n = 4 for CsA + HAMC and HAMC). The stroke infarct area was defined as the area lacking regular $NeuN^+$ staining in the ipsilateral hemisphere, using the contralateral hemisphere as a reference. The area in each section was measured using ImageJ software and the infarct volume between sections was calculated using the average area of damage between sections multiplied by the inter-section distance. The total infarct volume between AP +5 mm and AP −1.0 mm was calculated by summing the infarct volume between sections.

2.15. Ki67 and DCX pixel count

The number of $Ki67^+$ pixels in the lateral ventricles of the ipsilateral and contralateral hemispheres was counted in 4 coronal sections: AP +1.15, +0.5, 0.0 and −0.5 mm, relative to bregma. Z-stack images (5 μm step size) were taken with a 20× objective on a confocal microscope with a motorized stage, transformed into maximum projection images and stitched together. Each ventricle was imaged using consistent microscope settings. DAPI staining was used to identify and isolate the dorsoventral walls of the ventricles in the acquired images in ImageJ software. The "Default" threshold algorithm was used to set $Ki67^+$ pixels to white and $Ki67^-$ pixels to black. The total number of white pixels in the dorsoventral walls was automatically counted using ImageJ. Pixel counts for each coronal region and hemisphere were normalized to the average value of the untreated group. The overall pixel count for each hemisphere was the average of these normalized values across the 4 coronal sections. Identical analysis was carried out for DCX^+ pixels in the lateral ventricles.

2.16. Migratory DCX cell count

The number of migratory DCX cells located in the stroke penumbra, ipsilateral striatum and corpus callosum were manually counted on a fluorescence microscope using a 20× objective lens. All counts were performed in a blinded fashion. Cells were only counted if they were co-localized with DAPI nuclear staining and were clearly located outside the tightly clustered population of cells along the ventricles. Thus, the population of cells counted did not overlap with the population of cells quantified by the pixel counts. One significant outlier was removed from the HAMC treated group (final group sizes: n = 5 for untreated, n = 6 for CsA + HAMC, n = 4 for HAMC).

2.17. Statistics

Results are reported as mean + standard deviation. Statistical analyses were performed using Prism 6.0 (GraphPad Software Inc.). Significant outliers were detected with the Grubb's outlier test ($\alpha = 0.05$). Significance levels in figures are indicated by: $^*p < 0.05$; $^{**}p < 0.01$; $^{***}p < 0.001$; and $^{****}p < 0.0001$. Differences between two groups were compared with a two-tailed unpaired Student's t-test. Multiple groups were compared with a one-way ANOVA except for the organ exposure of CsA (Fig. 3B), where multiple t-tests were used. Multiple comparisons over time between two groups were performed using a two-way ANOVA. The Holm–Sidak post-hoc correction was used for all multiple comparisons. Reported p-values are adjusted for multiple-comparisons, where appropriate.

3. Results

3.1. In vivo release of CsA from HAMC in stroke-injured rat brains

Rat forebrain NSPCs are located 2.5 to 4.5 mm below the cortical surface. To determine if CsA delivered from epi-cortically injected HAMC diffuses to this NSPC niche in stroke-injured rats, we quantified in vivo release and tissue penetration in the brain. Animals were given an Et-1 induced stroke in the motor cortex and then HAMC containing CsA-loaded PLGA microparticles was injected onto the cortical surface (Fig. 1). Whole brain tissue was harvested at 1, 4, 7 and 14 days after implantation. Serial dorsoventral sections, 0.5 mm thick, were collected from the ipsilateral hemisphere and the CsA concentration in each section was measured using HPLC/MS–MS. Previous studies demonstrate the increased stability and modulus of PLGA-loaded HAMC [43], suggesting that CsA was released from the PLGA microparticles into HAMC from where it diffused into stroke-injured brain tissue, reaching a depth of 6 mm below the brain surface (Fig. 2A–D). The average concentration in the brain was highest 1 day post-implantation and decreased with time (Fig. 2E, $F_{3,16} = 9.121$, $p = 0.0009$). Importantly, CsA penetrated to the NSPC niche at all time points and CsA concentration in the NSPC niche (Fig. 2A–D, highlighted) did not significantly vary across time ($F_{3,16} = 1.896$, $p = 0.1710$).

At the time of sacrifice, the HAMC gel was collected from each animal and analyzed for the amount of remaining CsA. The linear decrease of CsA remaining in HAMC (data not shown) corresponded with the monotonic decrease in average concentration in the brain (Fig. 2E). The difference between the initial amount delivered and the amount remaining was used to calculate CsA release from HAMC in vivo (Fig. 2F). Linear regression analysis through the mean values ($r^2 = 0.9826$) calculated an average release rate of 1.481 μg CsA/day over 14 days. These results demonstrate that sustained CsA delivery to the stroke-injured rat brain is feasible with epi-cortically injected HAMC.

3.2. Comparison of CsA delivery by HAMC to conventional systemic delivery

To gain greater insight into local vs. systemic CsA delivery, the CsA concentration in the stroke-injured rat brain was measured and compared between the two techniques. Systemically administered CsA is able to cross the BBB due to its size and hydrophobicity. Using the sensory-motor cortex Et-1 stroke injury, systemically treated rats had a subcutaneous osmotic minipump implanted, which delivered a conventional dose of 12 mg CsA/kg/day over 14 days [6,31,32]. Brain tissue

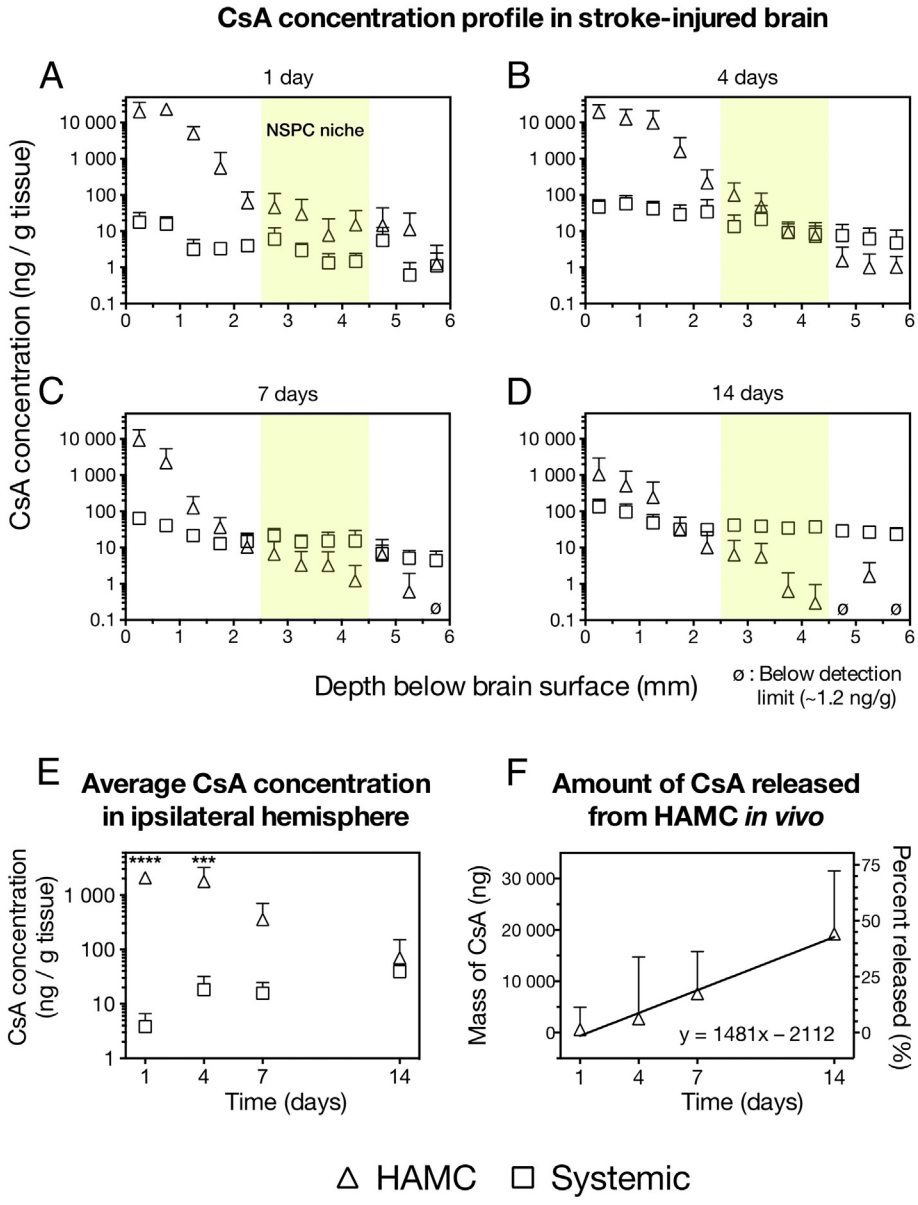

Fig. 2. Epi-cortical CsA delivery from HAMC-PLGA composite (HAMC, Δ, n = 5) provides sustained release to the stroke injured rat brain. CsA systemically delivered with a subcutaneous osmotic minipump (systemic, □, n = 4) diffuses across the BBB into the brain at similar levels throughout the depths examined. CsA penetration and spatial distribution in the ipsilateral hemisphere of stroke-injured rats was examined using HPLC–MS/MS after delivery for (A) 1 day, (B) 4 days, (C) 7 days and (D) 14 days (mean + standard deviation reported). CsA diffuses from HAMC to the NSPC niche located 2.5 to 4.5 mm from the brain surface (A–D, highlighted in yellow). Systemic delivery provided similar concentrations to the NSPC niche but required approximately 1000+ times more CsA released than the epi-cortical HAMC delivery system. (E) The average CsA concentration in the brain tissue was higher with HAMC delivery at all time points, with significant differences at 1 day ($p < 0.0001$) and 4 days ($p = 0.0002$). (F) Regression analysis on CsA released from HAMC (n = 5 per time point) showed CsA release in vivo was linear ($r^2 = 0.9826$). (For interpretation of the references to color in this figure legend, the reader is referred to the web version of this article.)

was harvested 1, 4, 7 and 14 days after implantation and the CsA concentration in 0.5 mm dorsoventral segments was measured using HPLC/MS–MS (Fig. 2A–D). CsA accumulated in the brain (Fig. 2E) and NSPC niche (Fig. 2A–D, highlighted) of systemically-treated rats at similar concentrations throughout the 6 mm depth examined.

Compared to systemic delivery, epi-cortically injected HAMC (Fig. 2E) provided substantially higher levels of CsA to the stroke-injured brain ($F_{1,28} = 31.02$, $p < 0.0001$). The differences varied over time ($F_{3,28} = 6.937$, $p = 0.0012$) and were most pronounced at 1 day ($p < 0.0001$) and 4 days ($p = 0.0002$). CsA concentration in the NSPC niche did not significantly vary between delivery methods ($F_{1,28} = 0.0012$, $p = 0.9722$) or over time ($F_{3,28} = 0.8439$, $p = 0.4815$).

The performance of HAMC and the minipump was also evaluated by their delivery efficiency, defined as the percentage of total administered drug found in the brain (Fig. 3A). HAMC used 1400 times less drug yet was 2700 to 876,000 times more efficient at CsA delivery than systemic delivery, which was enormously inefficient with only trace amounts of CsA found in the brain. These differences are significant ($F_{1,28} = 26.01$, $p < 0.0001$) and persisted over time ($F_{3,28} = 6.18$, $p = 0.0023$), being most pronounced at 1 d ($p < 0.0001$) and 4 d ($p = 0.0011$) post-implantation. Thus, HAMC proved to be a superior method for drug delivery to the brain by efficiently providing more CsA to the stroke-injured brain and equivalent levels to the NSPC niche while substantially lowering the dose delivered.

3.3. Organ exposure to CsA after delivery with HAMC

Systemic toxicity and immunosuppression are major concerns with CsA therapy, especially in stroke patients with stroke-induced immunodepression [44,45]. Here we evaluated CsA exposure to

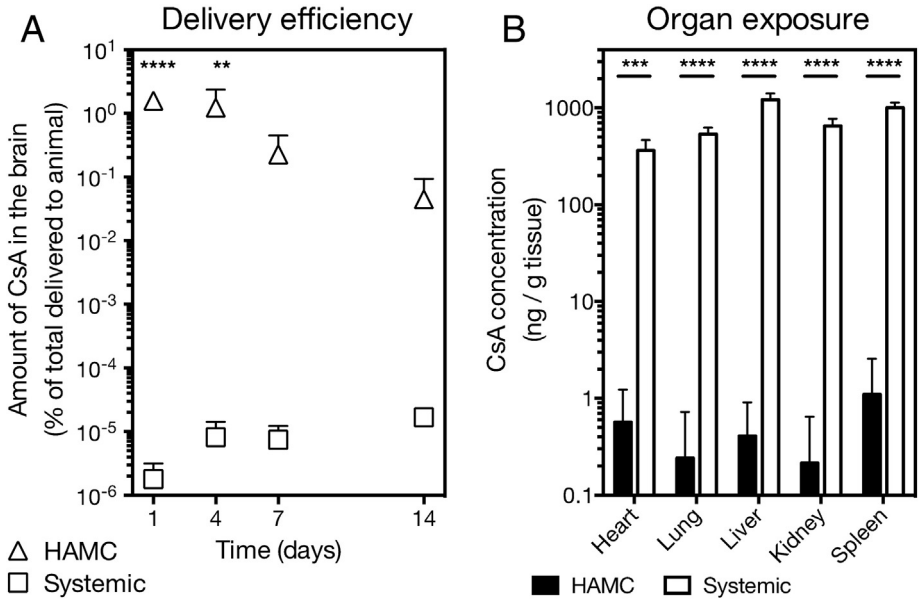

Fig. 3. Epi-cortical delivery from HAMC (△, n = 5) is more efficient than delivery from a subcutaneous osmotic minipump (□, n = 4) in terms of drug delivery to the brain and reduced systemic exposure (mean + standard deviation reported). (A) Efficiency was calculated as the amount of CsA found in the brain as a percentage of the total amount administered. Delivery with HAMC was orders of magnitude more efficient than delivery with a subcutaneous minipump, with significant differences at 1 day ($p < 0.0001$) and 4 days ($p = 0.0011$). (B) Organ exposure to CsA after release for 7 days is greatly reduced when delivered with HAMC (■, n = 4) compared to a subcutaneous minipump (□, n = 5). Differences were significant in all organs tested ($p = 0.0002$ for heart, $p < 0.0001$ for other organs).

non-CNS organs of stroke-injured rats after 7 days of drug release (Fig. 3B) from epi-cortically implanted HAMC and subcutaneous implanted minipumps. Samples of heart, lung, liver, kidney, and spleen were collected after sacrifice and CsA concentrations measured by HPLC/MS–MS. CsA delivery from HAMC resulted in little to no systemic drug exposure. In contrast, delivery with the minipump resulted in widespread CsA exposure at levels greater than that found in the brain, with the highest concentrations in the liver and spleen. In comparison, local delivery with HAMC markedly decreased systemic exposure in all organs evaluated ($p = 0.0002$ for heart, $p < 0.0001$ for remaining organs), with reductions ranging from 600 to 3000 times lower than with the minipump. Thus local delivery of CsA in HAMC to the brain is promising as it is minimally invasive, minimally systemically toxic, and enormously efficient as compared to systemic delivery and as demonstrated in this rat model of stroke.

3.4. Effect of CsA delivered from HAMC on stroke infarct volume

We investigated the biological effects of epi-cortical CsA delivery from HAMC on stroke-injured rats. Animals were given an endothelin-1 stroke in the sensory-motor cortex and immediately treated with: HAMC containing CsA-loaded PLGA microparticles (CsA + HAMC), vehicle HAMC containing blank PLGA microparticles (HAMC) or no treatment (Untreated). At 7 days post-injury the animals were sacrificed and coronal brain sections were processed for immunohistochemical staining.

First, we evaluated the effect of CsA released from HAMC on the stroke lesion. Coronal brain sections were stained with NeuN for mature neurons with DAPI as a nuclear counterstain. The loss of $NeuN^+$ staining after stroke injury was used to indicate the area of damaged tissue (representative images for untreated, CsA + HAMC treated and HAMC treated animals are shown in Fig. 4A). The area of damaged tissue in the ipsilateral hemisphere of serial sections was used to calculate the infarct volume between AP +5.0 and AP −1.0, relative to bregma.

Et-1 injection into the rat sensory-motor cortex led to stroke-infarct formation in all groups (Fig. 4B). The infarct volume was significantly reduced ($F_{2,10} = 7.236$, $p = 0.0114$) in both CsA + HAMC ($p = 0.0226$) and HAMC ($p = 0.0217$) treated groups compared to untreated animals. CsA treatment did not further decrease stroke infarct volume compared to the HAMC vehicle alone ($p = 0.8144$), demonstrating tissue sparing associated with HAMC itself.

3.5. Effect of CsA delivered from HAMC on endogenous NSPCs

We investigated the effect of local CsA release on endogenous forebrain NSPCs in stroke-injured rats. Coronal brain sections from injured animals that received no treatment, CsA + HAMC treatment or HAMC treatment for 7 days were co-stained with Ki67 for proliferating cells and DCX for neuronal progenitors, and DAPI as a nuclear counterstain. Cell proliferation in the NSPC niche (Fig. 5A–C) was quantified by the number of $Ki67^+$ pixels along the dorsolateral wall of ventricles in both cerebral hemispheres (Fig. 5D). $Ki67^+$ cell counts were performed on a subset of sections and correlated with pixel counts to confirm the method's validity (Supp. Fig. 1). The ventricles of 4 coronal sections around the Et-1 injection sites were analyzed per animal. Similar analysis was carried out for DCX^+ pixel counts along the ventricles; however, no significant difference was seen (data not shown).

CsA + HAMC treatment significantly enhanced the number of proliferating cells in the dorsolateral ventricular walls (Fig. 5E, $F_{2,15} = 6.979$, $p = 0.0072$), with a 1.32 fold increase compared to untreated animals ($p = 0.006$) and a 1.11 fold increase compared to HAMC treated animals ($p = 0.118$). Interestingly, when the hemispheres were analyzed individually, CsA + HAMC treatment significantly increased the number of proliferating cells not only on the ipsilateral ventricles (1.41 fold increase vs. untreated, $p = 0.0347$) but also the contralateral ventricles (1.22 fold increase vs. untreated, $p = 0.0150$; and 1.15 fold increase vs. HAMC, $p = 0.0551$). HAMC treated animals had no significant increase compared to untreated animals ($p = 0.106$).

Additionally, we examined whether CsA increased the number of NSPC progeny outside the ventricles. Migratory DCX^+ neuronal progenitors were counted in the stroke penumbra, in the ipsilateral striatum and the corpus callosum. These cells were distinguished by extending processes and were present as single cells rather than clusters of circular cells such as those found in the ventricles (Fig. 6A–C). Although

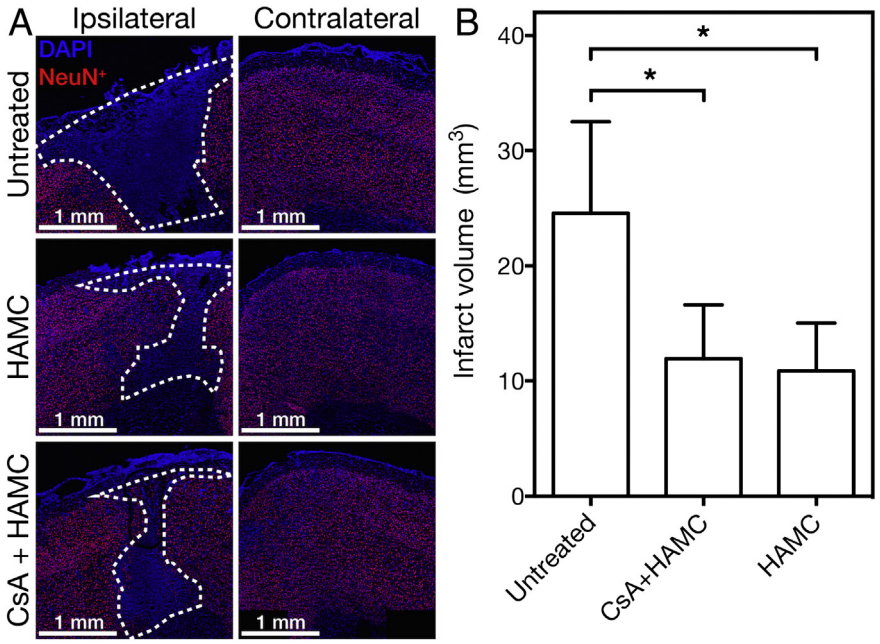

Fig. 4. HAMC reduces cerebral infarction after stroke. (A) Representative images of stroke infarct and neuron loss after stroke for untreated, CsA + HAMC treated and HAMC treated animals with damaged area outlined based on loss of $NeuN^+$ (red) staining, against DAPI (blue) background for cell bodies, compared to the contralateral hemisphere. (B) Quantification of the infarct volume in the ipsilateral hemisphere between AP +5.0 and AP −1.0 (mean + standard deviation reported, n = 5 for untreated, n = 4 for each of CsA + HAMC and HAMC). Both CsA + HAMC ($p = 0.0226$) and HAMC ($p = 0.0217$) significantly reduced stroke infarct volume compared to untreated controls. (For interpretation of the references to color in this figure legend, the reader is referred to the web version of this article.)

CsA + HAMC treated animals had more migratory neuronal progenitors (1.54 fold increase vs. untreated; and 1.68 fold increase vs. HAMC), the differences were not statistically significant due to the large variability in the CsA + HAMC group (Fig. 6D).

Thus, CsA released from HAMC can increase the number of proliferating cells in the NSPC niche, suggesting an increase in the number of proliferating NSPCs, and may increase the number of migratory neuronal progenitors. Taken together these results indicate that local delivery of CsA with HAMC is able to stimulate endogenous NSPCs in stroke-injured rat brain, consistent with the pro-survival effect that CsA has been shown to have on mouse NSPCs [31–34].

4. Discussion

Epi-cortical drug delivery from HAMC has been previously shown as a versatile platform for local therapeutic delivery to the mouse brain. Both hydrophilic proteins and hydrophobic drugs can be delivered in a controlled manner, with timescales ranging from days

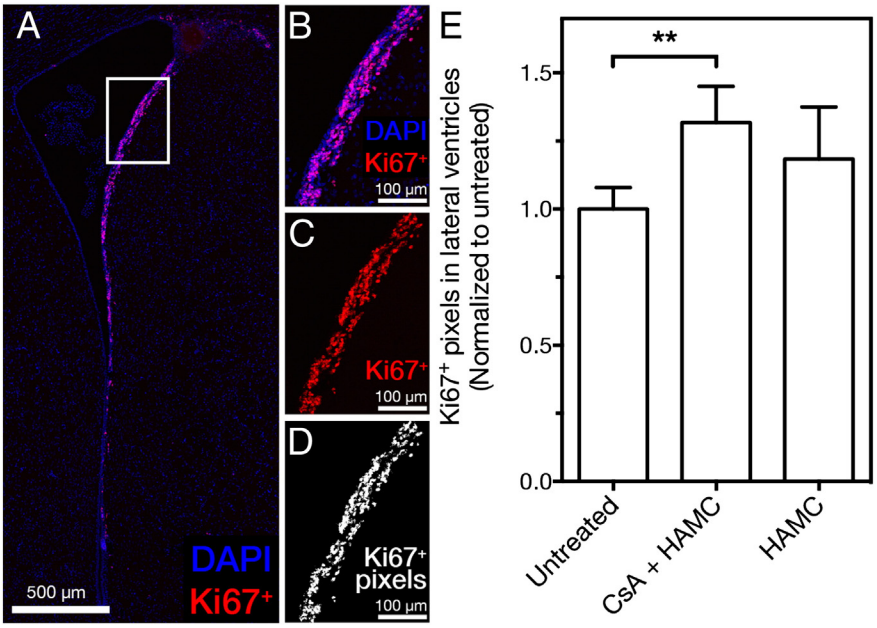

Fig. 5. Epi-cortical delivery of CsA from HAMC increased the amount of $Ki67^+$ proliferating cells in the lateral ventricles of stroke-injured rats. Representative images of $Ki67^+$ staining of cells along the lateral ventricles (A,B) with and (C) without DAPI staining. (D) The number of $Ki67^+$ pixels along the dorsolateral ventricle wall was used to quantify the number of $Ki67^+$ cells in both cerebral hemispheres (mean + standard deviation reported, n = 5 for untreated, n = 7 for CsA + HAMC, n = 6 for HAMC). Only treatment with CsA + HAMC significantly increased the $Ki67^+$ signal in the ventricles ($p = 0.006$ vs. untreated).

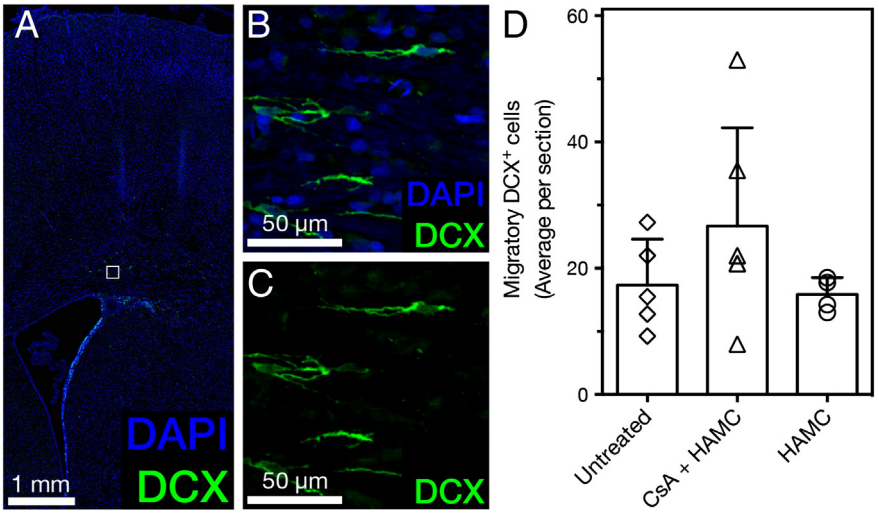

Fig. 6. Epi-cortical delivery of CsA from HAMC increased the presence of migratory neuronal progenitors (DCX^+) in stroke-injured rats. (A–C) Representative images of DCX^+ migratory neuroblasts in the stroke penumbra. (D) Quantitative comparison of the average number of DCX^+ cells in the stroke penumbra, ipsilateral striatum and the corpus callosum (mean + standard deviation reported, n = 5 for untreated, n = 6 for CsA + HAMC and n = 4 for HAMC). Treatment with CsA shows a trend toward increased numbers of DCX^+ cells (1.54 fold increase vs. untreated; and 1.68 fold increase vs. HAMC).

[12,13] to weeks [7,15]. One of the questions is whether this strategy can be translated to larger brains. In a step toward answering this question, we examined local epi-cortical delivery in the stroke-injured rat brain, which is 4-times the volume of the mouse brain.

We demonstrate that epi-cortically injected HAMC can be used for local CsA administration to, the Et-1 stroke injured rat brain, providing sustained CsA release and sufficient tissue penetration for delivery to the sub-cortical NSPC niche for at least 14 days. The in vivo release rate of CsA is slower than its in vitro release rate and is consistent with previous results in mice [15]. Drug release from HAMC is diffusion mediated [15,46] yet when PLGA particles are dispersed in HAMC, the burst release typically seen from PLGA particles alone [47] is attenuated [15,48]. In vitro drug release is an idealized case where sink conditions are maintained to maximize the driving force for Fickian diffusion and parameters that hinder diffusion in vivo are non-existent. Transport through the brain occurs in a tortuous ($\lambda = 1.6$ to 1.8) [49] and narrow pathway (38 to 64 nm between cells) [50] within the limited extracellular space (ECS) that comprises only 20% of the total brain volume [51,52]. Increased viscosity of the interstitial fluid and extracellular matrix (ECM) interactions also hinder drug movement [49,53]. These factors result in the reduction of CsA's apparent diffusivity within the ECS and its diffusion through brain tissue, thereby reducing diffusion-mediated release in vivo.

Several conditions in the stroke-injured brain further hinder diffusion and tissue penetration. Post-stroke cytotoxic edema of neurons and astrocytes [54] causes the ECS to shrink (from 20% to 5% of total brain volume) and tortuosity to increase (from $\lambda = 1.6$–1.8 to $\lambda \approx 2.1$) [55], resulting in slower diffusion [56]. Drug elimination from the brain ECS reduces tissue penetration and occurs in several pathways: transport into the circulation, binding to ECM components and receptors, uptake by other cells, and catabolism [57]. The BBB becomes leaky after stroke, increasing drug permeability and elimination via circulation [58]. Increased cellular infiltration into the stroke lesion also increases elimination [59] as small lipophilic molecules like CsA readily cross the lipidic cell membrane. Acidosis [60] and catabolic enzymes [61] in the stroke-injured tissue affect drug stability. Thus, in uninjured or chronically injured tissue, CsA's tissue penetration should be greater than we measured in acute stroke-injured tissue due to the increased extracellular volume for transport and decreased elimination.

Interestingly, HAMC alone reduced the infarct volume when applied after stroke, significantly reducing the lesion size relative to untreated controls, without the need for additional drugs. This finding is consistent with previous results in mice where HAMC [13] and HAMC with PLGA particles [7] reduced the stroke cavity volume, number of reactive astrocytes and activated microglia at 7, 18 and 32 days after stroke. The hyaluronan in HAMC is anti-inflammatory, inhibiting leukocyte migration [62] and inflammation [63]. In the CNS, HA has wound healing and anti-inflammatory properties after TBI [64] and spinal cord injury [9,65]. The attenuated inflammation after HAMC treatment may account for the reduced infarct volume observed [59]. Interestingly, CsA did not provide any additional reduction in infarct volume despite substantially higher doses reaching the injured tissue compared with systemic delivery. In previous studies, CsA's neuroprotective effects after systemic delivery were shown to be independent of immunomodulatory effects [66,67], directly promoting neuronal survival [68,69]. In this study, the stronger effects of HAMC may have masked any neuroprotection afforded by CsA. This is a promising finding for the treatment of stroke, as protection was achieved independent of any drug.

Notwithstanding the beneficial effects of HAMC, only with CsA delivery did the pool of proliferating cells in the NSPC niche increase at 7 days after stroke in the rat brain. Interestingly, CsA stimulated endogenous NSPCs in both hemispheres, indicating that CsA crossed over to the contralateral hemisphere. This may have resulted from a combination of diffusion across the longitudinal fissure separating the hemispheres and convective transport through the ventricular system via the circulating cerebrospinal fluid. We observed an increase in proliferating cells in the forebrain NSPC niche that likely results from a pro-survival effect rather than a change in growth kinetics [32–34]. Live cell imaging in vitro demonstrated that CsA increased the number of NSPC-derived neurospheres by promoting the survival of individual stem cells rather than modifying their proliferation kinetics [34]. CsA is known to promote NSPC survival in a calcineurin-independent fashion [32] through binding to cyclophilin D in the mitochondrial matrix [70], thereby inhibiting the opening of the mitochondrial permeability transition pore (MPTP) and preventing release of pro-apoptotic cytochrome C [71]. This pro-survival mechanism is not exclusive to NSPCs, as CsA is protective in the brain [2,3,5,6,35,36,66–69], heart [72] and liver [73,74], reflecting the ubiquity of MPTP inhibition in cell survival [75,76]. Thus, CsA is a promising molecule for promoting NSPC survival in the stroke-injured brain.

The lack of safe and effective methods for drug delivery to the brain is a major hurdle for the development of stroke treatments [77–82].

Systemic delivery is only possible with a small number of drugs and, as we have demonstrated, only a very small fraction of the total drug accumulates in the brain. Additionally, drug efflux from the brain severely limits diffusion therein [39,40,83,84]. The majority of the drug delivered is dispersed throughout the body, as we observed, and thereby increases the risk of undesirable side effects and systemic toxicity. Blood brain barrier disruption is one proposed solution to address these issues [85,86], but it is neither practical nor safe for sustained, long term treatment [87]. Local delivery is necessary [85,88] but current methods are often ineffective [89] and dangerous [7,8]. HAMC is the proposed solution for less invasive drug delivery for endogenous brain repair [7,9,12,13,15,48]. As we demonstrated, HAMC reduces cerebral infarction and can effectively provide local and sustained drug delivery for endogenous neural stem and progenitor cell stimulation [7,12,13,15]. The ability to deliver drugs in an effective and protective manner with HAMC promises to lead to strategies that maximize recovery.

5. Conclusions

Here we demonstrate the clear advantages of HAMC-mediated local drug delivery to the brain. Epi-cortically injected HAMC provides sustained CsA release over 14 days in vivo, with sufficient tissue penetration to reach the sub-cortical NSPC niche. Compared to systemic delivery, local delivery with HAMC results in higher CsA concentrations in the brain and markedly reduced exposure to other organs of the body while utilizing substantially less drug. HAMC alone provides tissue protection in the injured CNS while locally released CsA stimulates endogenous NSPCs. The advent of safe and effective methods for local drug delivery, such as that provided with HAMC, opens the way for new therapeutic strategies for endogenous brain repair and recovery after stroke.

Supplementary data to this article can be found online at http://dx.doi.org/10.1016/j.jconrel.2015.07.023.

Author contributions

A.T. — concept and design, performed surgeries, collection and assembly of data, data analysis and interpretation; C.M.M. — concept and design, data interpretation; M.S.S. — concept and design, data analysis and interpretation. All authors contributed toward preparation and final approval of manuscript.

Conflict of interest

The authors declare no competing financial interests.

Acknowledgments

We are grateful to Michelle Young at the AIMS Laboratory, Matthew J. Caicco and Dr. Shawn C. Owen for development of and assistance with the HPLC–MS/MS protocol. We acknowledge funding from the Heart and Stroke Foundation (CMM, MSS), the Centre for Stroke Recovery (CMM, MSS, AT), Ontario Graduate Scholarship (AT), and CIHR Training Program in Regenerative Medicine (AT). The authors would like to thank Dr. Michael J. Cooke, Dr. Tobias Führmann, Jennifer S.A. Logie, Jaclyn M. Obermeyer, Ahil N. Ganesh, Nikolaos Mitrousis, Irja Elliot Donaghue, Priya N. Anandakumaran and M. Cecilia Alvarez-Veronesi for scientific discussions and manuscript feedback.

References

[1] Y. Chen, G. Dalwadi, H.A.E. Benson, Drug delivery across the blood–brain barrier, Curr. Drug Deliv. 1 (2004) 361–376.
[2] H. Uchino, E. Elmér, K. Uchino, P.A. Li, Q.P. He, M.L. Smith, et al., Amelioration by cyclosporin A of brain damage in transient forebrain ischemia in the rat, Brain Res. 812 (1998) 216–226.
[3] H. Uchino, E. Elmér, K. Uchino, O. Lindvall, B.K. Siesjö, Cyclosporin A dramatically ameliorates CA1 hippocampal damage following transient forebrain ischaemia in the rat, Acta Physiol. Scand. 155 (1995) 469–471, http://dx.doi.org/10.1111/j.1748-1716.1995.tb09999.x.
[4] T. Yoshimoto, B.K. Siesjö, Posttreatment with the immunosuppressant cyclosporin A in transient focal ischemia, Brain Res. 839 (1999) 283–291.
[5] H. Friberg, M. Ferrand-Drake, F. Bengtsson, A.P. Halestrap, T. Wieloch, Cyclosporin A, but not FK 506, protects mitochondria and neurons against hypoglycemic damage and implicates the mitochondrial permeability transition in cell death, J. Neurosci. 18 (1998) 5151–5159.
[6] P.G. Sullivan, M. Thompson, S.W. Scheff, Continuous infusion of cyclosporin A postinjury significantly ameliorates cortical damage following traumatic brain injury, Exp. Neurol. 161 (2000) 631–637, http://dx.doi.org/10.1006/exnr.1999.7282.
[7] Y. Wang, M.J. Cooke, N. Sachewsky, C.M. Morshead, M.S. Shoichet, Bioengineered sequential growth factor delivery stimulates brain tissue regeneration after stroke, J. Control. Release 172 (2013) 1–11, http://dx.doi.org/10.1016/j.jconrel.2013.07.032.
[8] P.A. Mead, J.E. Safdieh, P. Nizza, S. Tuma, K.A. Sepkowitz, Ommaya reservoir infections: a 16-year retrospective analysis, J. Infect. 68 (2014) 225–230, http://dx.doi.org/10.1016/j.jinf.2013.11.014.
[9] D. Gupta, C.H. Tator, M.S. Shoichet, Fast-gelling injectable blend of hyaluronan and methylcellulose for intrathecal, localized delivery to the injured spinal cord, Biomaterials 27 (2006) 2370–2379, http://dx.doi.org/10.1016/j.biomaterials.2005.11.015.
[10] C.E. Kang, P.C. Poon, C.H. Tator, M.S. Shoichet, A new paradigm for local and sustained release of therapeutic molecules to the injured spinal cord for neuroprotection and tissue repair, Tissue Eng. A. 15 (2009) 595–604, http://dx.doi.org/10.1089/ten.tea.2007.0349.
[11] C.E. Kang, C.H. Tator, M.S. Shoichet, Poly(ethylene glycol) modification enhances penetration of fibroblast growth factor 2 to injured spinal cord tissue from an intrathecal delivery system, J. Control. Release 144 (2010) 25–31, http://dx.doi.org/10.1016/j.jconrel.2010.01.029.
[12] M.J. Cooke, Y. Wang, C.M. Morshead, M.S. Shoichet, Controlled epi-cortical delivery of epidermal growth factor for the stimulation of endogenous neural stem cell proliferation in stroke-injured brain, Biomaterials 32 (2011) 5688–5697, http://dx.doi.org/10.1016/j.biomaterials.2011.04.032.
[13] Y. Wang, M.J. Cooke, C.M. Morshead, M.S. Shoichet, Hydrogel delivery of erythropoietin to the brain for endogenous stem cell stimulation after stroke injury, Biomaterials 33 (2012) 2681–2692, http://dx.doi.org/10.1016/j.biomaterials.2011.12.031.
[14] C.E. Kang, M.D. Baumann, C.H. Tator, M.S. Shoichet, Localized and sustained delivery of fibroblast growth factor-2 from a nanoparticle-hydrogel composite for treatment of spinal cord injury, Cells Tissues Organs (Print) 197 (2013) 55–63, http://dx.doi.org/10.1159/000339589.
[15] M.J. Caicco, M.J. Cooke, Y. Wang, A. Tuladhar, C.M. Morshead, M.S. Shoichet, A hydrogel composite system for sustained epi-cortical delivery of Cyclosporin A to the brain for treatment of stroke, J. Control. Release 166 (2013) 197–202, http://dx.doi.org/10.1016/j.jconrel.2013.01.002.
[16] D. Lloyd-Jones, R.J. Adams, T.M. Brown, M. Carnethon, S. Dai, G. De Simone, et al., Heart disease and stroke statistics—2010 update: a report from the American Heart Association, Circulation 121 (2010) e46–e215, http://dx.doi.org/10.1161/CIRCULATIONAHA.109.192667.
[17] S. Weiss, B.A. Reynolds, A.L. Vescovi, C. Morshead, C.G. Craig, D. van der Kooy, Is there a neural stem cell in the mammalian forebrain? Trends Neurosci. 19 (1996) 387–393.
[18] P.S. Eriksson, E. Perfilieva, T. Björk-Eriksson, A.M. Alborn, C. Nordborg, D.A. Peterson, et al., Neurogenesis in the adult human hippocampus, Nat. Med. 4 (1998) 1313–1317, http://dx.doi.org/10.1038/3305.
[19] T. Yamashita, M. Ninomiya, P. Hernández Acosta, J.M. García-Verdugo, T. Sunabori, M. Sakaguchi, et al., Subventricular zone-derived neuroblasts migrate and differentiate into mature neurons in the post-stroke adult striatum, J. Neurosci. 26 (2006) 6627–6636, http://dx.doi.org/10.1523/JNEUROSCI.0149-06.2006.
[20] A. Arvidsson, T. Collin, D. Kirik, Z. Kokaia, O. Lindvall, Neuronal replacement from endogenous precursors in the adult brain after stroke, Nat. Med. 8 (2002) 963–970, http://dx.doi.org/10.1038/nm747.
[21] K. Jin, X. Wang, L. Xie, X.O. Mao, W. Zhu, Y. Wang, et al., Evidence for stroke-induced neurogenesis in the human brain, Proc. Natl. Acad. Sci. U. S. A. 103 (2006) 13198–13202, http://dx.doi.org/10.1073/pnas.0603512103.
[22] C.M. Morshead, C.G. Craig, D. van der Kooy, In vivo clonal analyses reveal the properties of endogenous neural stem cell proliferation in the adult mammalian forebrain, Development 125 (1998) 2251–2261.
[23] D.N. Abrous, M. Koehl, M. Le Moal, Adult neurogenesis: from precursors to network and physiology, Physiol. Rev. 85 (2005) 523–569, http://dx.doi.org/10.1152/physrev.00055.2003.
[24] C.T. Ekdahl, J.-H. Claasen, S. Bonde, Z. Kokaia, O. Lindvall, Inflammation is detrimental for neurogenesis in adult brain, Proc. Natl. Acad. Sci. U. S. A. 100 (2003) 13632–13637, http://dx.doi.org/10.1073/pnas.2234031100.
[25] C. Wiltrout, B. Lang, Y. Yan, R.J. Dempsey, R. Vemuganti, Repairing brain after stroke: a review on post-ischemic neurogenesis, Neurochem. Int. 50 (2007) 1028–1041, http://dx.doi.org/10.1016/j.neuint.2007.04.011.
[26] T. Teramoto, J. Qiu, J.-C. Plumier, M.A. Moskowitz, EGF amplifies the replacement of parvalbumin-expressing striatal interneurons after ischemia, J. Clin. Invest. 111 (2003) 1125–1132, http://dx.doi.org/10.1172/JCI17170.
[27] B. Kolb, C. Morshead, C. Gonzalez, M. Kim, C. Gregg, T. Shingo, et al., Growth factor-stimulated generation of new cortical tissue and functional recovery after stroke damage to the motor cortex of rats, J. Cereb. Blood Flow Metab. 27 (2007) 983–997, http://dx.doi.org/10.1038/sj.jcbfm.9600402.
[28] L. Belayev, L. Khoutorova, K.L. Zhao, A.W. Davidoff, A.F. Moore, S.C. Cramer, A novel neurotrophic therapeutic strategy for experimental stroke, Brain Res. 1280 (2009) 117–123, http://dx.doi.org/10.1016/j.brainres.2009.05.030.

[29] R.J. Dempsey, K.A. Sailor, K.K. Bowen, K. Türeyen, R. Vemuganti, Stroke-induced progenitor cell proliferation in adult spontaneously hypertensive rat brain: effect of exogenous IGF-1 and GDNF, J. Neurochem. 87 (2003) 586–597.

[30] K. Jin, Y. Zhu, Y. Sun, X.O. Mao, L. Xie, D.A. Greenberg, Vascular endothelial growth factor (VEGF) stimulates neurogenesis in vitro and in vivo, Proc. Natl. Acad. Sci. U. S. A. 99 (2002) 11946–11950, http://dx.doi.org/10.1073/pnas.182296499.

[31] A. Erlandsson, C.-H.A. Lin, F. Yu, C.M. Morshead, Immunosuppression promotes endogenous neural stem and progenitor cell migration and tissue regeneration after ischemic injury, Exp. Neurol. 230 (2011) 48–57, http://dx.doi.org/10.1016/j.expneurol.2010.05.018.

[32] N. Sachewsky, J. Hunt, M.J. Cooke, A. Azimi, T. Zarin, C. Miu, et al., Cyclosporin A enhances neural precursor cell survival in mice through a calcineurin-independent pathway, Dis. Model Mech. 7 (2014) 953–961, http://dx.doi.org/10.1242/dmm.014480.

[33] J. Hunt, A. Cheng, A. Hoyles, E. Jervis, C.M. Morshead, Cyclosporin A has direct effects on adult neural precursor cells, J. Neurosci. 30 (2010) 2888–2896, http://dx.doi.org/10.1523/JNEUROSCI.5991-09.2010.

[34] J. Hunt, C. Morshead, Cyclosporin A enhances cell survival in neural precursor populations in the adult central nervous system, Mol. Cell. Pharmacol. 2 (2010) 81–88.

[35] Y. Shiga, H. Onodera, Y. Matsuo, K. Kogure, Cyclosporin A protects against ischemia–reperfusion injury in the brain, Brain Res. 595 (1992) 145–148.

[36] Z. Xie, B. Lei, Q. Huang, J. Deng, M. Wu, W. Shen, et al., Neuroprotective effect of Cyclosporin A on the development of early brain injury in a subarachnoid hemorrhage model: a pilot study, Brain Res. 1472 (2012) 113–123, http://dx.doi.org/10.1016/j.brainres.2012.06.053.

[37] W.T. Cefalu, W.M. Pardridge, Restrictive transport of a lipid-soluble peptide (cyclosporin) through the blood–brain barrier, J. Neurochem. 45 (1985) 1954–1956, http://dx.doi.org/10.1111/j.1471-4159.1985.tb10557.x.

[38] D.J. Begley, L.K. Squires, B.V. Zloković, D.M. Mitrović, C.C. Hughes, P.A. Revest, et al., Permeability of the blood–brain barrier to the immunosuppressive cyclic peptide cyclosporin A, J. Neurochem. 55 (1990) 1222–1230, http://dx.doi.org/10.1111/j.1471-4159.1990.tb03128.x.

[39] A. Sakata, I. Tamai, K. Kawazu, Y. Deguchi, T. Ohnishi, A. Saheki, et al., In vivo evidence for ATP-dependent and P-glycoprotein-mediated transport of cyclosporin A at the blood–brain barrier, Biochem. Pharmacol. 48 (1994) 1989–1992, http://dx.doi.org/10.1016/0006-2952(94)90601-7.

[40] A.H. Schinkel, E. Wagenaar, L. van Deemter, C.A. Mol, P. Borst, Absence of the mdr1a P-Glycoprotein in mice affects tissue distribution and pharmacokinetics of dexamethasone, digoxin, and cyclosporin A, J. Clin. Invest. 96 (1995) 1698–1705, http://dx.doi.org/10.1172/JCI118214.

[41] G. Akdemir, M.F. Ergüngör, M. Sezer, L. Albayrak, E. Dağlioğlu, K. Kilinç, Therapeutic efficacy of intraventricular cyclosporine A and methylprednisolone on a global cerebral ischemia model in rats, Neurol. Res. 27 (2005) 827–834, http://dx.doi.org/10.1179/016164105X63610.

[42] V. Windle, A. Szymanska, S. Granter-Button, C. White, R. Buist, J. Peeling, et al., An analysis of four different methods of producing focal cerebral ischemia with endothelin-1 in the rat, Exp. Neurol. 201 (2006) 324–334, http://dx.doi.org/10.1016/j.expneurol.2006.04.012.

[43] M.D. Baumann, C.E. Kang, C.H. Tator, M.S. Shoichet, Intrathecal delivery of a polymeric nanocomposite hydrogel after spinal cord injury, Biomaterials 31 (2010) 7631–7639, http://dx.doi.org/10.1016/j.biomaterials.2010.07.004.

[44] U. Dirnagl, J. Klehmet, J.S. Braun, H. Harms, C. Meisel, T. Ziemssen, et al., Stroke-Induced Immunodepression: Experimental Evidence and Clinical Relevance, Stroke 38 (2007) 770–773, http://dx.doi.org/10.1161/01.STR.0000251441.89665.bc.

[45] A. Vogelgesang, A. Dressel, Immunological consequences of ischemic stroke: Immunosuppression and autoimmunity, J. Neuroimmunol. 231 (2011) 105–110, http://dx.doi.org/10.1016/j.jneuroim.2010.09.023.

[46] Y. Wang, Y. Lapitsky, C.E. Kang, M.S. Shoichet, Accelerated release of a sparingly soluble drug from an injectable hyaluronan–methylcellulose hydrogel, J. Control. Release 140 (2009) 218–223, http://dx.doi.org/10.1016/j.jconrel.2009.05.025.

[47] X. Huang, C.S. Brazel, On the importance and mechanisms of burst release in matrix-controlled drug delivery systems, J. Control. Release 73 (2001) 121–136, http://dx.doi.org/10.1016/S0168-3659(01)00248-6.

[48] M.D. Baumann, C.E. Kang, J.C. Stanwick, Y. Wang, H. Kim, Y. Lapitsky, et al., An injectable drug delivery platform for sustained combination therapy, J. Control. Release 138 (2009) 205–213, http://dx.doi.org/10.1016/j.jconrel.2009.05.009.

[49] E. Syková, C. Nicholson, Diffusion in brain extracellular space, Physiol. Rev. 88 (2008) 1277–1340, http://dx.doi.org/10.1152/physrev.00027.2007.

[50] R.G. Thorne, C. Nicholson, In vivo diffusion analysis with quantum dots and dextrans predicts the width of brain extracellular space, Proc. Natl. Acad. Sci. U. S. A. 103 (2006) 5567–5572, http://dx.doi.org/10.1073/pnas.0509425103.

[51] C. Nicholson, J.M. Phillips, Ion diffusion modified by tortuosity and volume fraction in the extracellular microenvironment of the rat cerebellum, J. Physiol. 321 (1981) 225–257.

[52] C. Nicholson, E. Syková, Extracellular space structure revealed by diffusion analysis, Trends Neurosci. 21 (1998) 207–215.

[53] R.G. Thorne, A. Lakkaraju, E. Rodriguez-Boulan, C. Nicholson, In vivo diffusion of lactoferrin in brain extracellular space is regulated by interactions with heparan sulfate, Proc. Natl. Acad. Sci. U. S. A. 105 (2008) 8416–8421, http://dx.doi.org/10.1073/pnas.0711345105.

[54] D. Liang, S. Bhatta, V. Gerzanich, J.M. Simard, Cytotoxic edema: mechanisms of pathological cell swelling, Neurosurg. Focus. 22 (2007) E2.

[55] I. Vorísek, E. Syková, Ischemia-induced changes in the extracellular space diffusion parameters, K+, and pH in the developing rat cortex and corpus callosum, J. Cereb. Blood Flow Metab. 17 (1997) 191–203, http://dx.doi.org/10.1097/00004647-199702000-00009.

[56] D.K. Binder, M.C. Papadopoulos, P.M. Haggie, A.S. Verkman, In vivo measurement of brain extracellular space diffusion by cortical surface photobleaching, J. Neurosci. 24 (2004) 8049–8056, http://dx.doi.org/10.1523/JNEUROSCI.2294-04.2004.

[57] W.M. Saltzman, M.L. Radomsky, Drugs released from polymers: diffusion and elimination in brain tissue, Chem. Eng. Sci. 46 (1991) 2429–2444.

[58] K.E. Sandoval, K.A. Witt, Blood–brain barrier tight junction permeability and ischemic stroke, Neurobiol. Dis. 32 (2008) 200–219, http://dx.doi.org/10.1016/j.nbd.2008.08.005.

[59] R. Jin, G. Yang, G. Li, Inflammatory mechanisms in ischemic stroke: role of inflammatory cells, J. Leukoc. Biol. 87 (2010) 779–789, http://dx.doi.org/10.1189/jlb.1109766.

[60] U. Dirnagl, C. Iadecola, M.A. Moskowitz, Pathobiology of ischaemic stroke: an integrated view, Trends Neurosci. 22 (1999) 391–397.

[61] E.H. Lo, X. Wang, M.L. Cuzner, Extracellular proteolysis in brain injury and inflammation: role for plasminogen activators and matrix metalloproteinases, J. Neurosci. Res. 69 (2002) 1–9, http://dx.doi.org/10.1002/jnr.10270.

[62] J.V. Forrester, P.C. Wilkinson, Inhibition of leukocyte locomotion by hyaluronic acid, J. Cell Sci. 48 (1981) 315–331.

[63] C.A. Cooper, K.K. Brown, C.D. Meletis, N. Zabriskie, Inflammation and Hyaluronic Acid, Altern. Complement. Ther. 14 (2008) 78–84, http://dx.doi.org/10.1089/act.2008.14201.

[64] S. Hou, Q. Xu, W. Tian, F. Cui, Q. Cai, J. Ma, et al., The repair of brain lesion by implantation of hyaluronic acid hydrogels modified with laminin, J. Neurosci. Methods 148 (2005) 60–70, http://dx.doi.org/10.1016/j.jneumeth.2005.04.016.

[65] J.W. Austin, C.E. Kang, M.D. Baumann, L. DiDiodato, K. Satkunendrarajah, J.R. Wilson, et al., The effects of intrathecal injection of a hyaluronan-based hydrogel on inflammation, scarring and neurobehavioural outcomes in a rat model of severe spinal cord injury associated with arachnoiditis, Biomaterials 33 (2012) 4555–4564, http://dx.doi.org/10.1016/j.biomaterials.2012.03.022.

[66] A.S. Korde, L.C. Pettigrew, S.D. Craddock, C.B. Pocernich, P.C. Waldmeier, W.F. Maragos, Protective Effects of NIM811 in Transient Focal Cerebral Ischemia Suggest Involvement of the Mitochondrial Permeability Transition, J. Neurotrauma 24 (2007) 895–908, http://dx.doi.org/10.1089/neu.2006.0122.

[67] L.H.A.N. Mbye, I.N. Singh, K.M. Carrico, K.E. Saatman, E.D. Hall, Comparative neuroprotective effects of cyclosporin A and NIM811, a nonimmunosuppressive cyclosporin A analog, following traumatic brain injury, J. Cereb. Blood Flow Metab 29 (2009) 87–97, http://dx.doi.org/10.1038/jcbfm.2008.93.

[68] K. Domańska-Janik, L. Buzańska, J. Dłużniewska, H. Kozłowska, A. Sarnowska, B. Zabłocka, Neuroprotection by cyclosporin A following transient brain ischemia correlates with the inhibition of the early efflux of cytochrome C to cytoplasm, Mol. Brain Res. 121 (2004) 50–59, http://dx.doi.org/10.1016/j.molbrainres.2003.11.006.

[69] M. Kawakami, Molecular Dissection of Cyclosporin A's Neuroprotective Effect Reveals Potential Therapeutics for Ischemic Brain Injury, Brain Sci. 3 (2013) 1325–1356, http://dx.doi.org/10.3390/brainsci3031325.

[70] C.P. Baines, R.A. Kaiser, N.H. Purcell, N.S. Blair, H. Osinska, M.A. Hambleton, et al., Loss of cyclophilin D reveals a critical role for mitochondrial permeability transition in cell death, Nature 434 (2005) 658–662, http://dx.doi.org/10.1038/nature03434.

[71] E. Basso, L. Fante, J. Fowlkes, V. Petronilli, M.A. Forte, P. Bernardi, Properties of the permeability transition pore in mitochondria devoid of Cyclophilin D, J. Biol. Chem. 280 (2005) 18558–18561, http://dx.doi.org/10.1074/jbc.C500089200.

[72] A.P. Halestrap, S.J. Clarke, S.A. Javadov, Mitochondrial permeability transition pore opening during myocardial reperfusion—a target for cardioprotection, Cardiovasc. Res. 61 (2004) 372–385, http://dx.doi.org/10.1016/S0008-6363(03)00533-9.

[73] Y. Masubuchi, S. Kano, T. Horie, Mitochondrial permeability transition as a potential determinant of hepatotoxicity of antidiabetic thiazolidinediones, Toxicology 222 (2006) 233–239, http://dx.doi.org/10.1016/j.tox.2006.02.017.

[74] N.C. Teoh, G.C. Farrell, Hepatic ischemia reperfusion injury: pathogenic mechanisms and basis for hepatoprotection, J. Gastroenterol. Hepatol. 18 (2003) 891–902, http://dx.doi.org/10.1046/j.1440-1746.2003.03056.x.

[75] J.J. Lemasters, A.-L. Nieminen, T. Qian, L.C. Trost, S.P. Elmore, Y. Nishimura, et al., The mitochondrial permeability transition in cell death: a common mechanism in necrosis, apoptosis and autophagy, Biochim. Biophys. Acta Bioenerg. 1366 (1998) 177–196, http://dx.doi.org/10.1016/S0005-2728(98)00112-1.

[76] J.-S. Kim, L. He, J.J. Lemasters, Mitochondrial permeability transition: a common pathway to necrosis and apoptosis, Biochem. Biophys. Res. Commun. 304 (2003) 463–470, http://dx.doi.org/10.1016/S0006-291X(03)00618-1.

[77] M.D. Hill, R.H. Martin, D. Mikulis, J.H. Wong, F.L. Silver, K.G. Terbrugge, et al., Safety and efficacy of NA-1 in patients with iatrogenic stroke after endovascular aneurysm repair (ENACT): a phase 2, randomised, double-blind, placebo-controlled trial, Lancet Neurol. 11 (2012) 942–950, http://dx.doi.org/10.1016/S1474-4422(12)70225-9.

[78] H. Ehrenreich, K. Weissenborn, H. Prange, D. Schneider, C. Weimar, K. Wartenberg, et al., Recombinant human erythropoietin in the treatment of acute ischemic stroke, Stroke 40 (2009) e647–e656, http://dx.doi.org/10.1161/STROKEAHA.109.564872.

[79] I. Sayeed, D.G. Stein, Progesterone as a neuroprotective factor in traumatic and ischemic brain injury, Prog. Brain Res. 175 (2009) 19-19, http://dx.doi.org/10.1016/S0079-6123(09)17515-5.

[80] V.E. O'Collins, M.R. Macleod, G.A. Donnan, L.L. Horky, B.H. van der Worp, D.W. Howells, 1,026 experimental treatments in acute stroke, Ann. Neurol. 59 (2006) 467–477, http://dx.doi.org/10.1002/ana.20741.

[81] A. Rogalewski, A. Schneider, E.B. Ringelstein, W.-R. Schäbitz, Toward a multimodal neuroprotective treatment of stroke, Stroke 37 (2006) 1129–1136, http://dx.doi.org/10.1161/01.STR.0000209330.73175.34.

[82] F.D. Miller, D.R. Kaplan, Mobilizing endogenous stem cells for repair and regeneration: are we there yet? Cell Stem Cell 10 (2012) 650–652, http://dx.doi.org/10.1016/j.stem.2012.05.004.

[83] A.H. Schinkel, P-Glycoprotein, a gatekeeper in the blood–brain barrier, Adv. Drug Deliv. Rev. 36 (1999) 179–194, http://dx.doi.org/10.1016/S0169-409X(98)00085-4.

[84] W. Löscher, H. Potschka, Blood–brain barrier active efflux transporters: ATP-binding cassette gene family, NeuroRx 2 (2005) 86–98, http://dx.doi.org/10.1602/neurorx.2.1.86.
[85] A. Misra, S. Ganesh, A. Shahiwala, S.P. Shah, Drug delivery to the central nervous system: a review, J. Pharm. Pharm. Sci. 6 (2003) 252–273.
[86] K. Hynynen, N. McDannold, N.A. Sheikov, F.A. Jolesz, N. Vykhodtseva, Local and reversible blood–brain barrier disruption by noninvasive focused ultrasound at frequencies suitable for trans-skull sonications, NeuroImage 24 (2005) 12–20, http://dx.doi.org/10.1016/j.neuroimage.2004.06.046.
[87] S. Krol, Challenges in drug delivery to the brain: Nature is against us, J. Control. Release 164 (2012) 145–155, http://dx.doi.org/10.1016/j.jconrel.2012.04.044.
[88] W.M. Pardridge, Drug delivery to the brain, J. Cereb. Blood Flow Metab. 17 (1997) 713–731, http://dx.doi.org/10.1097/00004647-199707000-00001.
[89] W.M. Pardridge, Drug transport in brain via the cerebrospinal fluid, Fluids and Barriers of the CNS, 8 2011, p. 7, http://dx.doi.org/10.1186/2045-8118-8-7.